

MoRA: High-Rank Updating for Parameter-Efficient Fine-Tuning

Anonymous ACL submission

Abstract

Low-rank adaptation (LoRA) is a popular parameter-efficient fine-tuning (PEFT) method for large language models (LLMs). In this paper, we analyze the impact of low-rank updating, as implemented in LoRA. Our findings suggest that the low-rank updating mechanism may limit the ability of LLMs to effectively learn and memorize new knowledge. Inspired by this observation, we propose a new method called MoRA, which employs a square matrix to achieve high-rank updating while maintaining the same number of trainable parameters. To achieve it, we introduce the corresponding non-parameter operators to reduce the input dimension and increase the output dimension for the square matrix. Furthermore, these operators ensure that the weight can be merged back into LLMs, which makes our method can be deployed like LoRA. We perform a comprehensive evaluation of our method across five tasks: instruction tuning, mathematical reasoning, continual pretraining, memory and pre-training. Our method outperforms LoRA on memory-intensive tasks and achieves comparable performance on other tasks.

1 Introduction

As the size of language models increases, parameter-efficient fine-tuning (PEFT) (Houlsby et al., 2019) has emerged as a popular technique to adapt these models to specific downstream tasks. Compared to Full Fine-Tuning (FFT), which updates all model parameters, PEFT modifies only a small part of the parameters. For example, it can achieve similar performance with FFT by updating less than 1% of the parameters in some tasks (Hu et al., 2021), which significantly reduces the memory requirements for the optimizer and facilitates the storage and deployment of fine-tuned models.

Among the existing PEFT methods, Low-Rank Adaptation (LoRA) (Hu et al., 2021) is particularly prevalent for LLMs. LoRA enhances perfor-

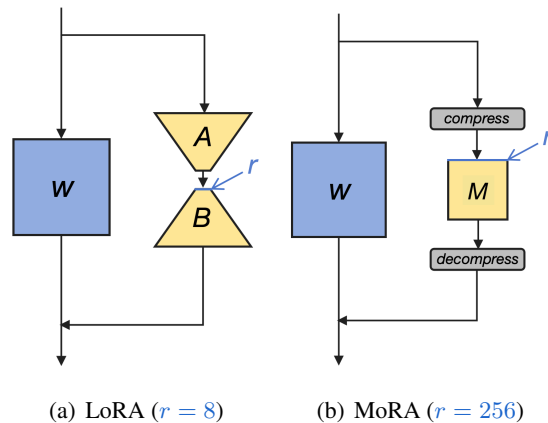


Figure 1: An overview of our method compared to LoRA under **same** number of trainable parameters. W is the frozen weight from model. A and B are trainable low-rank matrices in LoRA. M is the trainable matrix in our method. Gray parts are non-parameter operators to reducing the input dimension and increasing the output dimension. r represents the rank in two methods.

mance over other PEFT methods such as prompt tuning (Lester et al., 2021) or adapters (Houlsby et al., 2019) by updating parameters via low-rank matrices. These matrices can be merged into the original model parameters, thereby avoiding additional computational costs during inference. There are numerous methods that aim to improve LoRA for LLMs. However, most methods primarily validate their efficiency based on GLUE (Wang et al., 2018), either by achieving better performance or by requiring fewer trainable parameters. Recent methods (Liu et al., 2024; Meng et al., 2024; Zhu et al., 2024) leverage instruction tuning task such as Alpaca (Wang et al., 2024) or reasoning tasks like GSM8K (Cobbe et al., 2021) to better evaluate their performance on LLMs. However, the diverse settings and datasets used in the evaluation complicate the understanding of their progression.

In this paper, we conduct a comprehensive evaluation of LoRA across various tasks under the

062	same settings, including instruction tuning, mathe-	113
063	matical reasoning, and continual pretraining. We	114
064	find that LoRA-like methods demonstrate similar	115
065	performance across these tasks and they perform	116
066	comparably to FFT in instruction tuning but fall	
067	short in mathematical reasoning and continual pre-	
068	training. Among these tasks, instruction tuning	
069	primarily focuses on interacting with the format,	
070	rather than acquiring knowledge and capabilities,	
071	which are learned almost entirely during pretrain-	
072	ing (Zhou et al., 2024). We observe that LoRA	
073	is easily adapted to follow response formats in	
074	instruction tuning but struggles with other tasks	
075	that require enhancing knowledge and capabilities	
076	through fine-tuning.	
077	One plausible explanation for this limitation ob-	
078	served with LoRA could be its reliance on low-rank	
079	updates (Lialin et al., 2023). The low-rank update	
080	matrix, ΔW , struggles to estimate the full-rank	
081	updates in FFT, particularly in memory-intensive	
082	tasks like continual pretraining that require memo-	
083	rizing domain-specific knowledge. Since the rank	
084	of ΔW is significantly smaller than the full rank,	
085	this limitation restricts capacity to store new infor-	
086	mation via fine-tuning. Moreover, current variants	
087	of LoRA cannot alter the inherent characteristic of	
088	low-rank updates. To validate this, we conducted a	
089	memorization task using pseudo-data to assess the	
090	performance of LoRA in memorizing new knowl-	
091	edge. We found that LoRA performed significantly	
092	worse than FFT, even with a large rank such as 256.	
093	Given these observations, we introduce a method	
094	called MoRA, which employs a square matrix as	
095	opposed to low-rank matrices, aiming to maximize	
096	the rank in ΔW while maintaining the same num-	
097	ber of trainable parameters. For instance, when	
098	utilizing 8 rank with the hidden size 4096, LoRA	
099	employs two low-rank matrices $A \in \mathbb{R}^{4096 \times 8}$ and	
100	$B \in \mathbb{R}^{8 \times 4096}$, with $rank(\Delta W) \leq 8$. Under same	
101	number of parameters, our method uses a square	
102	matrix $M \in \mathbb{R}^{256 \times 256}$, with $rank(\Delta W) \leq 256$,	
103	as depicted in Figure 1. Notably, our method ex-	
104	hibits a greater capacity than LoRA with a large	
105	rank. To decrease the input dimension and increase	
106	the output dimension for M , we develop corre-	
107	sponding non-parameter operators. Furthermore,	
108	these operators and M can be substituted by a ΔW ,	
109	ensuring our method can be merged back into LLM	
110	like LoRA.	
111	Our contributions are as follows:	
112	1. We introduce MoRA, a novel method that em-	
	ploy a square matrix instead of low-rank ma-	113
	trices in LoRA to achieve high-rank updating,	114
	while maintaining the same number of train-	115
	able parameters.	116
	2. We discuss four kinds of non-parameter op-	117
	erators of MoRA to reduce the input dimen-	118
	sion and increase the output dimension for the	119
	square matrix, while ensures that the weight	120
	can be merged back into LLMs.	121
	3. We evaluate MoRA across five tasks: mem-	122
	ory, instruction tuning, mathematical reason-	123
	ing, continual pretraining, and pretraining.	124
	Our method outperforms LoRA on memory-	125
	intensive tasks and achieves comparable per-	126
	formance on other tasks, which demonstrates	127
	the effectiveness of high-rank updating.	128
	2 Related Work	129
	2.1 LoRA	130
	LoRA is one of the most popular PEFT methods	131
	for fine-tuning LLM, owing to its broad applicabil-	132
	ity and robust performance in comparison to other	133
	methods. To approximate the updated weight ΔW	134
	in FFT, LoRA employs two low-rank matrices for	135
	its decomposition. By adjusting the rank of these	136
	two matrices, LoRA can accordingly modify the	137
	trainable parameters. Benefit from it, LoRA can	138
	merge these matrices after fine-tuning without the	139
	inference latency compared to FFT. There are many	140
	methods to further improve LoRA, particularly for	141
	the application in LLMs. DoRA(Liu et al., 2024)	142
	further decomposes the original weight into mag-	143
	nitude and direction components and uses LoRA	144
	to update the direction component. LoRA+(Hayou	145
	et al., 2024) employs different learning rates for	146
	the two low-rank matrices to improve learning ef-	147
	iciency. ReLoRA(Lialin et al., 2023) integrates	148
	LoRA into the LLM during training to increase the	149
	rank of the final ΔW .	150
	2.2 Fine-Tuning with LLMs	151
	Despite the impressive performance of LLMs with	152
	in-context learning, certain scenarios still necessi-	153
	tate fine-tuning, which can be broadly categorized	154
	into three types. The first type, instruction tuning,	155
	aims to better align LLMs with end tasks and user	156
	preferences, without significantly enhancing the	157
	knowledge and capabilities of LLMs (Zhou et al.,	158
	2024). This approach simplifies the process of	159

dealing with varied tasks and understanding complex instructions. The second type involves complex reasoning tasks such as mathematical problem-solving (Collins et al., 2023; Imani et al., 2023; Yu et al., 2023), where general instruction tuning often falls short in handling complex, symbolic, multi-step reasoning tasks. To improve the reasoning abilities of LLMs, the majority of research focuses on creating corresponding training datasets, either by leveraging larger teacher models like GPT-4 (Fu et al., 2023), or by rephrasing questions along a reasoning path (Yu et al., 2023). The third type, continual pretraining (Cheng et al., 2023; Chen et al., 2023; Han et al., 2023; Liu et al., 2023), aims to enhance the domain-specific capabilities of LLMs. Unlike instruction tuning, it necessitates fine-tuning to augment the corresponding domain-specific knowledge and capabilities.

However, most variants of LoRA (Kopiczko et al., 2023; Lialin et al., 2023; Dettmers et al., 2024; Zhu et al., 2024) predominantly employ instruction tuning or text classification tasks from GLUE (Wang et al., 2018) to validate their efficacy on LLMs. Given that instruction tuning requires the least capacity for fine-tuning compared to other types, it may not accurately reflect the effectiveness of LoRA variants. To better evaluate their methods, recent works (Meng et al., 2024; Liu et al., 2024; Shi et al., 2024; Renduchintala et al., 2023) have employed reasoning tasks to test their methods. But the training sets used are often too small for LLMs to effectively learn reasoning. For instance, some methods (Meng et al., 2024; Renduchintala et al., 2023) utilize the GSM8K (Cobbe et al., 2021) with only 7.5K training samples. Compare to the SOTA method with 395K training samples (Yu et al., 2023), this small training set achieves worse performance on reasoning and makes it hard to evaluate the effectiveness of these methods.

3 Analysis the Influence of Low-rank Updating

The key idea of LoRA (Hu et al., 2021) involves the use of low-rank updates to estimate full-rank updates in FFT. Formally, given a pretrained parameter matrix $W_0 \in \mathbb{R}^{d \times k}$, LoRA employs two low-rank matrices to calculate the weight update ΔW :

$$h = W_0 x + \Delta W x = W_0 x + B A x \quad (1)$$

where $A \in \mathbb{R}^{r \times k}$ and $B \in \mathbb{R}^{d \times r}$ represent the low-rank matrices in LoRA. To ensure that $\Delta W = 0$

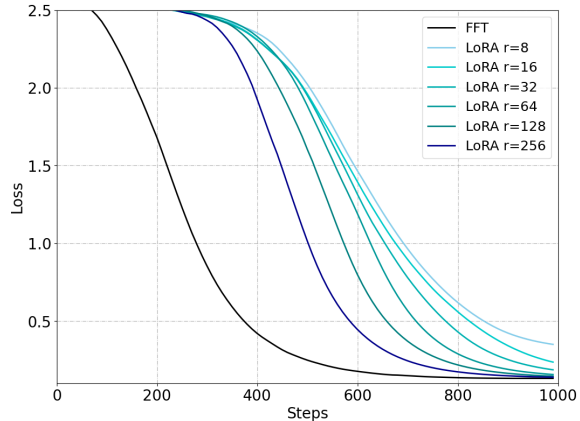


Figure 2: Performance of memorizing UUID pairs through fine-tuning with FFT and LoRA.

at the beginning of training, LoRA initializes A with a Gaussian distribution and B with zero. Due to the low-rank decomposition of ΔW into BA , the $rank(\Delta W) \leq r$. The weight update in LoRA exhibits a markedly low rank, $r \ll \min(d, k)$, in comparison to the full-rank updating in FFT. Low-rank updating by LoRA shows on-par performance with full-rank updating in some tasks such as text classification or instruction tuning (Liu et al., 2024; Meng et al., 2024). However, for tasks like complex reasoning or continual pretraining, LoRA tends to show worse performance (Liu et al., 2023).

Based on these observations, we propose a hypothesis that low-rank updating is easy to leverage original knowledge and capabilities of LLM to solve task, but it is struggle to handle tasks that require enhancing knowledge and capabilities of LLM.

To substantiate this hypothesis, we examine the differences between LoRA and FFT in terms of memorizing new knowledge through fine-tuning. In order to circumvent leveraging the original knowledge of the LLM, we randomly generate 10K pairs of Universally Unique Identifiers (UUIDs), each pair comprising two UUIDs with 32 hexadecimal values. The task requires the LLM to generate the corresponding UUID based on the input UUID. For instance, given a UUID such as “205f3777-52b6-4270-9f67-c5125867d358”, the model should generate the corresponding UUID based on 10K training pairs. This task can also be viewed as a question-answering task, while the knowledge indispensable for accomplishing it is exclusively from the training datasets rather than the LLM itself.

For the training settings, we employ LLaMA-2

7B as base model, utilizing 1,000 pairs per batch and conducting 100 epochs. For the LoRA, we apply low-rank matrices to all linear layers and search learning rate from $\{1e-4, 2e-4, 3e-4\}$ to enhance performances. We conduct the experiment on LoRA using various ranks $r \in \{8, 16, 32, 64, 128, 256\}$. For the FFT, we directly use a learning rate of $3e-5$. Based on Figure 2, we observe low-rank updating are hard to memorizing new knowledge compared to FFT. Although constantly increasing the rank of LoRA can alleviate this problem, the gap still exists.

In contrast to the memory task, we also evaluate the performance gap between LoRA and FFT on instruction tuning, which merely introduces new knowledge. Similar to previous results (Meng et al., 2024; Zhu et al., 2024), we also find that LoRA matches the performance of FFT with small rank $r = 8$ in Table 1. This indicates that LoRA can easily leverage the original knowledge of LLMs by fine-tuning like FFT.

4 Method

Based on the above analysis, we propose a new method to alleviate the negative effects of low-rank updating. The main idea of our method is to utilize the same trainable parameters as much as possible to achieve a higher rank in ΔW . Consider to the pretrained weight $W_0 \in \mathbb{R}^{d \times k}$, LoRA uses two low-rank matrices A and B with $(d+k)r$ total trainable parameters for rank r . Under same trainable parameters, a square matrix $M \in \mathbb{R}^{\hat{r} \times \hat{r}}$ where $\hat{r} = \lfloor \sqrt{(d+k)r} \rfloor$ can achieve the highest rank due to $r \ll \min(d, k)$.

To accomplish this, we need to reduce the input dimension and increase the output dimension for M . Formally,

$$h = W_0 x + f_{\text{decomp}}(M f_{\text{comp}}(x)) \quad (2)$$

where $f_{\text{comp}} : \mathbb{R}^k \rightarrow \mathbb{R}^{\hat{r}}$ denotes the function that decreases the input dimension of x from k to \hat{r} , and $f_{\text{decomp}} : \mathbb{R}^{\hat{r}} \rightarrow \mathbb{R}^d$ represents the function that enhances the output dimension from \hat{r} to d . Furthermore, these two functions ought to be non-parameterized operators and expected to execute in linear time corresponding to the dimension. They should also have corresponding function, $f_{\text{comp}} : \mathbb{R}^{\hat{r} \times \hat{r}} \rightarrow \mathbb{R}^{\hat{r} \times k}$ and $f_{\text{decomp}} : \mathbb{R}^{\hat{r} \times k} \rightarrow \mathbb{R}^{d \times k}$, to transform M into ΔW . For any x , the following should hold:

$$f_{\text{decomp}}(M f_{\text{comp}}(x)) = \Delta W x, \forall x \in \mathbb{R}^k \quad (3)$$

where $\Delta W = f_{\text{decomp}}(f_{\text{comp}}(M))$. If Eq. 3 holds, M can be losslessly expanded to ΔW based on f_{comp} and f_{decomp} . This allows our method to merge back into the LLM like LoRA.

For the design of f_{comp} and f_{decomp} , we explore several methods to implement these functions. One straightforward method is truncating the dimension and subsequently add it in corresponding dimension. Formally, this can be represented as:

$$\begin{aligned} f_{\text{comp}}(x) &= x_{1:\hat{r}} \\ f_{\text{decomp}}(x) &= \begin{bmatrix} x \\ \mathbf{0} \end{bmatrix} \end{aligned} \quad (4)$$

and the corresponding ΔW is:

$$\Delta W = \begin{bmatrix} M & \mathbf{0} \\ \mathbf{0} & \mathbf{0} \end{bmatrix} \quad (5)$$

However, this method leads to a significant loss of information during compression and only modifies a segment of the output by appending a zero vector during decompression. To improve it, we can share the rows and columns of M to achieve a more efficient compression and decompression. Formally, this can be represented as:

$$\begin{aligned} f_{\text{comp}}(x) &= [\sum_{j \in g_i} x_j]_{i=1}^r \\ f_{\text{decomp}}(x) &= [x_{\tilde{g}'_i}]_{i=1}^d \end{aligned} \quad (6)$$

Here, g and g' represent predefined groups that share the same row and column in M , respectively. The $j \in g_i$ indicates that the j -th dimension belongs to the i -th group in g . The term \tilde{g}'_i is the reverse of g'_i , referring to the i -th dimension associated with the \tilde{g}'_i -th group in g' . The corresponding ΔW is as follows:

$$\Delta W_{i,j} = M_{\tilde{g}'_i, \tilde{g}_j} \quad (7)$$

Sharing rows and columns can be efficient for larger ranks such as $r = 128$ or $r = 256$, as only a few rows or columns in ΔW share a common row or column. For instance, considering to $\Delta W \in \mathbb{R}^{4096 \times 4096}$ for $r = 128$, which has $\hat{r} = 1024$ and $M \in \mathbb{R}^{1024 \times 1024}$. In this situation, only 4 rows or columns share the same row or column. Conversely, for smaller ranks such as $r = 8$, where $\hat{r} = 256$, it requires average 16 rows or columns in a group to share the same row or column in M . It can lead to inefficiencies due to the significant information loss during compression in Eq. 6.

To enhance performance for smaller ranks, we reshape x instead of directly compressing it, to preserve the input information. In this context, $f_{\text{comp}}(x) : \mathbb{R}^k \rightarrow \mathbb{R}^{n \times \hat{r}}$ and $f_{\text{decomp}} : \mathbb{R}^{n \times \hat{r}} \rightarrow \mathbb{R}^d$. Corresponding f_{comp} , f_{decomp} and ΔW are as follows:

$$\begin{aligned} f_{\text{comp}}(x) &= [x_{1:\hat{r}} \quad x_{\hat{r}:2\hat{r}} \quad \cdots \quad x_{(n-1)\hat{r}:n\hat{r}}] \\ f_{\text{decomp}}(x) &= \text{concat}(x) \\ \Delta W &= \begin{bmatrix} M & \mathbf{0} & \cdots & \mathbf{0} \\ \mathbf{0} & M & \cdots & \mathbf{0} \\ \vdots & \vdots & \ddots & \vdots \\ \mathbf{0} & \mathbf{0} & \cdots & M \end{bmatrix} \end{aligned} \quad (8)$$

where $\text{concat}(x)$ refers to concatenate the rows of x into a vector. For simplicity, we omit the padding and truncation operators in above functions and focus on the case where $d = k$. In comparison to sharing columns and rows, this method incurs additional computational overhead by reshaping x into $\mathbb{R}^{n \times \hat{r}}$ instead of $\mathbb{R}^{\hat{r}}$. However, given that the size of M is significantly smaller than W_0 , this additional computation is very small for rank like 8. For instance, when fine-tuning the 7B model with rank of 8 ($\hat{r} = 256$), this method is only 1.03 times slower than previous methods.

Inspired by RoPE (Su et al., 2024), we can further refine this method by incorporating rotation operators into f_{comp} to augment the expressiveness of M by enable it to differentiate between various $x_{i\hat{r}:(i+1)\hat{r}}$ by rotating them. We can modify Eq. 8 as follows:

$$\begin{aligned} f_{\text{comp}}(x) &= [a^1 \quad a^2 \quad \cdots \quad a^{n-1}] \\ \Delta W &= \begin{bmatrix} P^1 & \mathbf{0} & \cdots & \mathbf{0} \\ \mathbf{0} & P^2 & \cdots & \mathbf{0} \\ \vdots & \vdots & \ddots & \vdots \\ \mathbf{0} & \mathbf{0} & \cdots & P^{n-1} \end{bmatrix} \end{aligned} \quad (9)$$

where a^i and P^i represent the corresponding values of $x_{i\hat{r}:(i+1)\hat{r}}$ and M post-rotation, respectively. Following RoPE, we use a $\hat{r} \times \hat{r}$ block diagonal matrix to achieve the rotation. However, our method use rotation information to enable M distinguish the $x_{i\hat{r}:(i+1)\hat{r}}$ instead of token position in RoPE. We can define a^i and P^i as follows:

$$\begin{aligned} a^i &= \begin{bmatrix} R_{\theta_{1,i}} & \mathbf{0} & \cdots & \mathbf{0} \\ \mathbf{0} & R_{\theta_{2,i}} & \cdots & \mathbf{0} \\ \vdots & \vdots & \ddots & \vdots \\ \mathbf{0} & \mathbf{0} & \cdots & R_{\theta_{\frac{\hat{r}}{2},i}} \end{bmatrix} x_{i\hat{r}:(i+1)\hat{r}} \\ P^i &= M \begin{bmatrix} R_{\theta_{1,i}} & \mathbf{0} & \cdots & \mathbf{0} \\ \mathbf{0} & R_{\theta_{2,i}} & \cdots & \mathbf{0} \\ \vdots & \vdots & \ddots & \vdots \\ \mathbf{0} & \mathbf{0} & \cdots & R_{\theta_{\frac{\hat{r}}{2},i}} \end{bmatrix} \end{aligned} \quad (10)$$

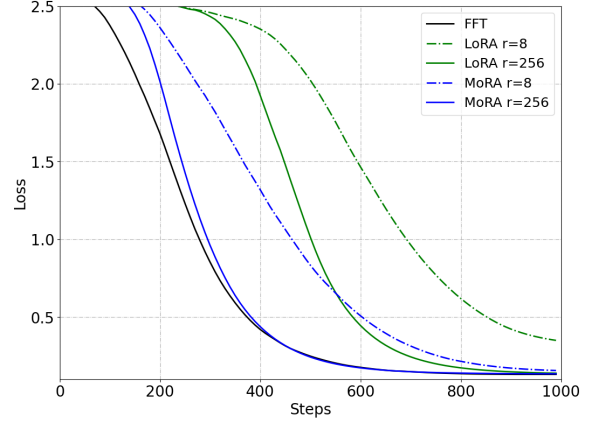


Figure 3: Performance of memorizing UUID pairs with LoRA and our method on rank 8 and 256.

where $\theta_j = 10000^{-2(j-1)/\hat{r}}$ and $R_{\theta_j,i} \in \mathbb{R}^{2 \times 2}$ is a rotation matrix:

$$R_{\theta_j,i} = \begin{bmatrix} \cos i\theta_j & -\sin i\theta_j \\ \sin i\theta_j & \cos i\theta_j \end{bmatrix} \quad (11)$$

5 Experiment

We evaluate our method on various tasks to understand the influence of high-rank updating. In Section 5.1, we evaluate our method with LoRA and our method on memorizing UUID pairs to show the benefit of high-rank updating on memorizing. In Section 5.2, we reproduce LoRA, LoRA variants and FFT on three fine-tuning tasks: instruction tuning, mathematical reasoning and continual pre-training. In Section 5.3, we compare our method with LoRA and ReLoRA on pretraining by training transformer from scratch.

5.1 Memorizing UUID Pairs

We first compare our method with LoRA and FFT on memorizing UUID pairs to demonstrate improvements through high-rank updating. Following the training settings in Section 3, we search learning rate from $\{5e-5, 1e-4, 2e-4\}$ and use decompress and compress functions in Eq. 8, sharing rows and columns in M . Due to use one matrix M instead of two matrices A and B , we can directly initialize M with zeros. For the predefined groups g and g' , we group every adjacent \hat{r} rows or columns together. The training loss is presented in Figure 3. Our method shows significant improvements over LoRA with the same number of trainable parameters, benefiting from high-rank updating. We also report character-level accuracy at various training steps in Table 2. MoRA requires fewer training steps to memorize these UUID pairs compared to

Method	Rank	Instruction Tuning		Mathematical Reasoning		Continual Pretraining	
		MMLU 0	MMLU 5	GSM8K	MATH	BioMed.	Finance
FFT	-	50.6	51.3	66.6	20.1	56.4	69.6
LoRA	8	50.2	51.5	64.6	15.1	52.3	64.0
LoRA+	8	49.2	51.1	64.1	15.8	52.2	64.9
ReLoRA	8	49.3	50.2	61.5	14.5	46.3	61.0
AsyLoRA	8	50.3	52.2	64.5	15.0	52.5	63.5
DoRA	8	50.2	51.5	64.5	14.6	52.5	63.9
MoRA (Ours)	8	49.7	51.5	64.2	15.4	53.3	67.1
LoRA	256	49.7	50.8	67.9	19.9	54.1	67.3
LoRA+	256	49.2	51.3	68.2	17.1	54.2	66.7
ReLoRA	256	-	-	64.0	18.1	52.9	57.9
AsyLoRA	256	50.1	52.0	66.9	19.3	54.1	66.9
DoRA	256	49.6	51.1	67.4	19.5	54.2	66.0
MoRA (Ours)	256	49.9	51.4	67.9	19.2	55.4	68.7

Table 1: Performance of FFT, LoRA, LoRA variants and our method on instruction tuning, mathematical reasoning and continual pretraining tasks.

	Rank	300	500	700	900
FFT	-	42.5	100	100	100
LoRA	8	9.9	10.0	10.7	54.2
MoRA	8	10.1	15.7	87.4	100
LoRA	256	9.9	70.6	100	100
MoRA	256	41.6	100	100	100

Table 2: Character-level accuracy of memorizing UUID pairs by generating the value of corresponding key in 300, 500, 700 and 900 training steps.

LoRA. Compared to FFT, MoRA with 256 rank can achieve similar performance and both method can memorize all UUID pairs in 500 steps.

5.2 Fine-tuning Tasks

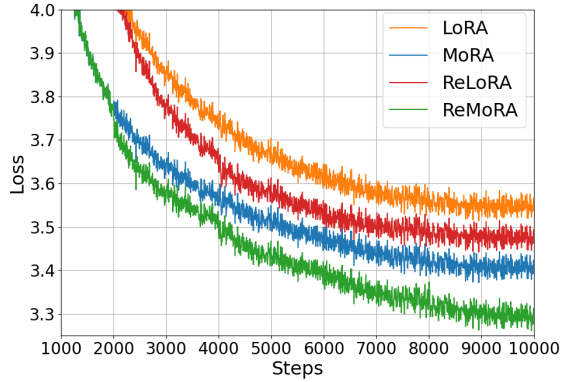
5.2.1 Setup

We evaluate our method across three fine-tuning tasks for large language models (LLMs): instruction tuning, mathematical reasoning, and continual pretraining. For these tasks, we select high-quality corresponding datasets to test both LoRA and our method. In instruction tuning, we utilize Tulu v2 (Iverson et al., 2023), a blend of several high-quality instruction datasets, containing 326k filtered samples. We assess instruction performance using the MMLU (Hendrycks et al., 2020) in both zero-shot and five-shot settings. For mathematical reasoning, we employ the MetaMath (Yu et al., 2023) with its 395k samples to enhance mathematical reasoning capabilities and also use GSM8K (Cobbe et al., 2021) and MATH (Hendrycks et al., 2021) for further evalu-

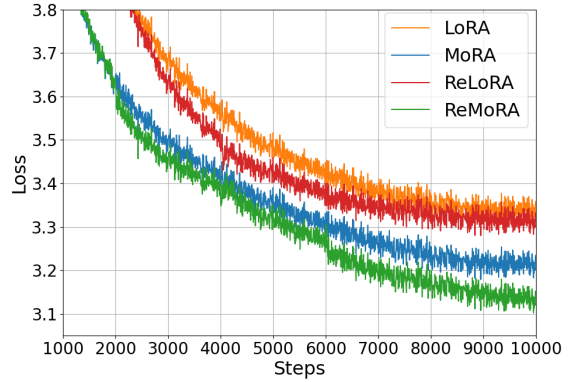
ation. In continual pretraining, we adapt an LLM to the biomedicine and finance using PubMed abstracts from the Pile (Gao et al., 2020) and financial news, complemented by data preprocessing methods from AdaptLLM (Cheng et al., 2023) to boost performance. We report the average performance of corresponding tasks for continual pretraining. More details can be found in Appendix C.

5.2.2 Baselines and Implements

For LoRA-like methods and MoRA, we conducted experiments at $r = 8$ and $r = 256$, and reproduce following methods across three tasks: FFT, LoRA, LoRA+ (Hayou et al., 2024), AsyLoRA (Zhu et al., 2024), ReLoRA (Lialin et al., 2023) and DoRA (Liu et al., 2024). LoRA+ enhances the learning rate of matrix B in LoRA to facilitate efficient feature learning based on theoretical analysis. We search the corresponding the hyperparameter λ from $\{2,4\}$. AsyLoRA also analyzes asymmetry in the A and B matrices, and we adopted their initialization strategy. ReLoRA proposes a method to merge low-rank matrices into the model during training to increase the rank of ΔW . we search merge steps from $\{1k, 2k\}$ and use 50 steps restarts warmup. DoRA leverages weight decomposition to enhance performance as a robust baseline. For FFT, we follow the settings proposed by corresponding datasets. For MoRA, we employed rotation operators as outlined in Eq. 9 to implement compression and decompression for $r = 8$, and for $r = 256$, we



(a) Pretraining loss at 250M models.



(b) Pretraining loss at 1.3B models.

Figure 4: Pretraining loss with LoRA and MoRA on 250M and 1B models from scratch. Both LoRA and MoRA use same amount of trainable parameters with $r = 128$. ReMoRA and ReLoRA refer to merge MoRA or LoRA back to the model during training to increase the rank of ΔW .

utilized shared rows and columns as specified in Eq. 6 and group every adjacent \hat{r} rows or columns together. The details hyperparameters about fine-tuning can be found in Appendix A.

5.2.3 Results and Analysis

We present the results of fine-tuning tasks in Table 1. We report the results of MMLU with zero-shot and 5-shot settings for instruction tuning, GSM8K and MATH for mathematical reasoning, and average performance on biomedical tasks and financial tasks for continual pretraining.

MoRA shows on par performances with LoRA on instruction tuning and mathematical reasoning. Benefit from high-rank updating to memorize new knowledge, MoRA outperforms LoRA on both biomedical and financial domains for continual pretraining.

We also find that LoRA variants exhibit similar performances on these fine-tuning tasks as compared to LoRA. Although AsyLoRA achieves the best performance in instruction tuning, it demonstrates poor performance in mathematical reasoning. For ReLoRA, merging low-rank matrices during training can harm performance, particularly at the high rank like 256.

Consider the difference between three tasks, they show different requirements for fine-tuning capabilities. For instruction tuning, which does not learn new knowledge from fine-tuning, rank 8 is enough to achieve performance similar to FFT. For mathematical reasoning, rank 8 is unable to match FFT performance. However, increasing the rank from 8 to 256 can eliminate the performance gap. For

	250M	1.3B
LoRA	33.40	28.56
MoRA (Ours)	28.54	25.25
ReLoRA	32.19	27.80
ReMoRA (Ours)	26.74	23.34

Table 3: Perplexity on C4 validation dataset.

continual pretraining, LoRA with rank 256 still underperforms FFT.

5.3 Pretraining

To understand the influence of high-rank updating, we train transformer from scratch on the C4 datasets (Raffel et al., 2020). For the model architecture, we train LLaMA-based model with RMSNorm (Zhang and Sennrich, 2019), SwiGLU (Shazeer, 2020) and RoPE (Su et al., 2024) on 250M and 1.3B sizes. For the hyperparameters, we use 10k steps, 1024 batch size, 512 sequence length and follow Lialin et al., using rank $r = 128$ for LoRA and our methods and also keep modules without applying LoRA-like layernorm or embeddings unfreezed. We compare our method with LoRA and ReLoRA. To better show the difference between high-rank and low-rank updating, we reproduce ReLoRA and other methods without full-rank training warmup. For MoRA, we use compression and decompression functions in Eq. 6 by sharing columns and rows.

We also combine merge-and-reint in ReLoRA with our method called ReMoRA by merging M back into the original parameters during training

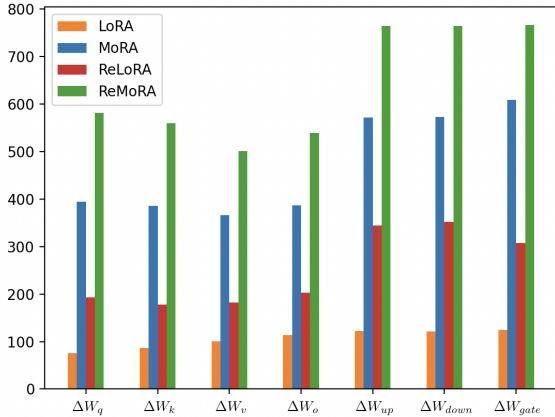


Figure 5: The number of singular values > 0.1 in ΔW on the 250M pretraining model.

to increase the rank of ΔW . However, if we directly merge M with g and g' in Eq. 6, the final rank of ΔW is unchanged due to the same expand pattern. To solve this problem, we can change g and g' after merging to ensure the rank of ΔW increasing. More details about ReMoRA can be found in Appendix B. For the hyperparameters corresponding to ReLoRA and ReMoRA, we merge every 2k steps and use 50 steps restarts warmup with optimizer resetting and jagged scheduler.

We show pretraining loss in Figure 4 and corresponding perplexity on C4 validation dataset in Table 3. Our method show better performance on pretraining compared to LoRA and ReLoRA with same amount of trainable parameters. Benefiting from high-rank updating, ReMoRA also achieves more improvements on MoRA compared to ReLoRA, which demonstrates the effectiveness of merge-and-reint strategy in ReMoRA.

6 Analysis

6.1 High-rank Updating

To demonstrate the impact of high-rank updating on the rank of ΔW , we analyzed the spectrum of singular values for the learned ΔW on 250M pretraining 250M model. We present the average count of singular values exceeding 0.1 across all layers for ΔW_q , ΔW_k , ΔW_v , ΔW_o , ΔW_{up} , ΔW_{down} , and ΔW_{gate} in Figure 5 following (Lialin et al., 2023). MoRA and ReMoRA exhibit a substantially higher number of significant singular values compared to LoRA and ReLoRA, highlighting the effectiveness of our methods in increasing the rank of ΔW . We find the quantity of singular values shown in Figure 5 can be correlated with the perplexity metrics

listed in Table 3. Moreover, MoRA, without merge-and-reint strategy in ReLoRA and ReMoRA, can achieve a lower perplexity than ReLoRA along with a higher significant singular values.

6.2 Influence of Decompression and Compression

To explore the impact of decompression and compression functions in MoRA, we report the performance on GSM8K using various methods: truncation, sharing, decoupling, and rotation in Table 4. Among these methods, truncation shows the worst performance due to the significant information loss during compression. Sharing can achieve better performance than truncation by leveraging the shared rows or columns to preserve the input information. But in the case of $r = 8$, sharing shows worse performance than decouple and rotation due to the large number of sharing rows or columns, as we discussed in Section 4. Rotation is more efficient than decouple, due to the rotation information can help the square matrix to distinguish the input information.

	f_{comp}, f_{decomp}	$r = 8$	$r = 256$
Truncation	Eq. 4	59.5	66.6
Sharing	Eq. 6	62.5	67.9
Decouple	Eq. 8	63.6	67.8
Rotation	Eq. 9	64.2	67.9

Table 4: Influence of decompression and compression functions on $r = 8$ and $r = 256$ on GSM8K.

7 Conclusion

In this paper, we analyze the impact of low-rank updating through LoRA and observe that such updating struggles for memory-intensive tasks, which also limits current LoRA variants. To overcome this limitation, we introduce MoRA, a method that utilizes non-parameterized operators for high-rank updating. Within the MoRA framework, we explore various methods to implement decompression and compression functions. Performance comparisons indicate that MoRA matches LoRA in instruction tuning and mathematical reasoning, and exhibits superior performance in continual pretraining and memory tasks. Additionally, we conduct pretraining experiments to further demonstrate the effectiveness of high-rank updating and show superior results compared to ReLoRA.

8 Limitation

Despite MoRA outperforming LoRA on memory-intensive tasks, it achieves similar performance on instruction tuning and mathematical reasoning compared to LoRA. Regarding training time and GPU memory usage, MoRA uses almost the same time and memory, benefiting from the non-parameterized operators. However, for small ranks like 8, MoRA uses Eq. 9 to compress and decompress input features, which may make it approximately 1.15 times slower than LoRA during fine-tuning. For the design of compression and decompression functions, we only explore several methods, but there could be more effective methods to compress and decompress features, such as directly dropping unnecessary rows or columns or grouping rows or columns based on the feature distribution.

References

Wei Chen, Qiushi Wang, Zefei Long, Xianyin Zhang, Zhongtian Lu, Bingxuan Li, Siyuan Wang, Jiarong Xu, Xiang Bai, Xuanjing Huang, et al. 2023. Discfinllm: A chinese financial large language model based on multiple experts fine-tuning. *arXiv preprint arXiv:2310.15205*.

Zhiyu Chen, Shiyang Li, Charese Smiley, Zhiqiang Ma, Sameena Shah, and William Yang Wang. 2022. Convinqa: Exploring the chain of numerical reasoning in conversational finance question answering. *arXiv preprint arXiv:2210.03849*.

Daixuan Cheng, Shaohan Huang, and Furu Wei. 2023. Adapting large language models via reading comprehension. *arXiv preprint arXiv:2309.09530*.

Karl Cobbe, Vineet Kosaraju, Mohammad Bavarian, Mark Chen, Heewoo Jun, Lukasz Kaiser, Matthias Plappert, Jerry Tworek, Jacob Hilton, Reiichiro Nakano, et al. 2021. Training verifiers to solve math word problems. *arXiv preprint arXiv:2110.14168*.

Katherine M Collins, Albert Q Jiang, Simon Frieder, Lionel Wong, Miri Zilka, Umang Bhatt, Thomas Lukasiewicz, Yuhuai Wu, Joshua B Tenenbaum, William Hart, et al. 2023. Evaluating language models for mathematics through interactions. *arXiv preprint arXiv:2306.01694*.

Franck Dernoncourt and Ji Young Lee. 2017. Pubmed 200k rct: a dataset for sequential sentence classification in medical abstracts. *arXiv preprint arXiv:1710.06071*.

Tim Dettmers, Artidoro Pagnoni, Ari Holtzman, and Luke Zettlemoyer. 2024. Qlora: Efficient finetuning of quantized llms. *Advances in Neural Information Processing Systems*, 36.

Yao Fu, Hao Peng, Litu Ou, Ashish Sabharwal, and Tushar Khot. 2023. Specializing smaller language models towards multi-step reasoning. In *International Conference on Machine Learning*, pages 10421–10430. PMLR.

Leo Gao, Stella Biderman, Sid Black, Laurence Golding, Travis Hoppe, Charles Foster, Jason Phang, Horace He, Anish Thite, Noa Nabeshima, et al. 2020. The pile: An 800gb dataset of diverse text for language modeling. *arXiv preprint arXiv:2101.00027*.

Tianyu Han, Lisa C Adams, Jens-Michalis Papaioannou, Paul Grundmann, Tom Oberhauser, Alexander Löser, Daniel Truhn, and Keno K Bresssem. 2023. Medalpaca—an open-source collection of medical conversational ai models and training data. *arXiv preprint arXiv:2304.08247*.

Soufiane Hayou, Nikhil Ghosh, and Bin Yu. 2024. LoRA+: Efficient Low Rank Adaptation of Large Models. 3.

Dan Hendrycks, Collin Burns, Steven Basart, Andy Zou, Mantas Mazeika, Dawn Song, and Jacob Steinhardt. 2020. Measuring massive multitask language understanding. *arXiv preprint arXiv:2009.03300*.

Dan Hendrycks, Collin Burns, Saurav Kadavath, Akul Arora, Steven Basart, Eric Tang, Dawn Song, and Jacob Steinhardt. 2021. Measuring mathematical problem solving with the math dataset. *arXiv preprint arXiv:2103.03874*.

Neil Houlsby, Andrei Giurgiu, Stanislaw Jastrzebski, Bruna Morrone, Quentin De Laroussilhe, Andrea Gesmundo, Mona Attariyan, and Sylvain Gelly. 2019. Parameter-efficient transfer learning for nlp. In *International conference on machine learning*, pages 2790–2799. PMLR.

Edward J Hu, Yelong Shen, Phillip Wallis, Zeyuan Allen-Zhu, Yuanzhi Li, Shean Wang, Lu Wang, and Weizhu Chen. 2021. Lora: Low-rank adaptation of large language models. *arXiv preprint arXiv:2106.09685*.

Shima Imani, Liang Du, and Harsh Shrivastava. 2023. Mathprompter: Mathematical reasoning using large language models. *arXiv preprint arXiv:2303.05398*.

Hamish Ivison, Yizhong Wang, Valentina Pyatkin, Nathan Lambert, Matthew Peters, Pradeep Dasigi, Joel Jang, David Wadden, Noah A Smith, Iz Beltagy, et al. 2023. Camels in a changing climate: Enhancing lm adaptation with tulu 2. *arXiv preprint arXiv:2311.10702*.

Di Jin, Eileen Pan, Nassim Oufattole, Wei-Hung Weng, Hanyi Fang, and Peter Szolovits. 2021. What disease does this patient have? a large-scale open domain question answering dataset from medical exams. *Applied Sciences*, 11(14):6421.

688	Qiao Jin, Bhuwan Dhingra, Zhengping Liu, William Cohen, and Xinghua Lu. 2019. Pubmedqa: A dataset for biomedical research question answering. In <i>Proceedings of the 2019 Conference on Empirical Methods in Natural Language Processing and the 9th International Joint Conference on Natural Language Processing (EMNLP-IJCNLP)</i> , pages 2567–2577.	743
689		744
690		745
691		746
692		747
693		748
694		
695	Dawid Jan Kopiczko, Tijmen Blankevoort, and Yuki Markus Asano. 2023. Vera: Vector-based random matrix adaptation. <i>arXiv preprint arXiv:2310.11454</i> .	749
696		750
697		
698		
699	Brian Lester, Rami Al-Rfou, and Noah Constant. 2021. The power of scale for parameter-efficient prompt tuning. <i>arXiv preprint arXiv:2104.08691</i> .	751
700		752
701		753
702	Vladislav Lialin, Namrata Shivagunde, Sherin Muckatira, and Anna Rumshisky. 2023. Stack more layers differently: High-rank training through low-rank updates. <i>arXiv preprint arXiv:2307.05695</i> .	754
703		755
704		
705		
706	Mingjie Liu, Teodor-Dumitru Ene, Robert Kirby, Chris Cheng, Nathaniel Pinckney, Rongjian Liang, Jonah Alben, Himyanshu Anand, Sanmitra Banerjee, Ismet Bayraktaroglu, et al. 2023. Chipnemo: Domain-adapted llms for chip design. <i>arXiv preprint arXiv:2311.00176</i> .	756
707		757
708		758
709		759
710		760
711		761
712	Shih-Yang Liu, Chien-Yi Wang, Hongxu Yin, Pavlo Molchanov, Yu-Chiang Frank Wang, Kwang-Ting Cheng, and Min-Hung Chen. 2024. Dora: Weight-decomposed low-rank adaptation. <i>arXiv preprint arXiv:2402.09353</i> .	762
713		763
714		764
715		765
716		766
717	Macedo Maia, Siegfried Handschuh, André Freitas, Brian Davis, Ross McDermott, Manel Zarrouk, and Alexandra Balahur. 2018. Www’18 open challenge: financial opinion mining and question answering. In <i>Companion proceedings of the the web conference 2018</i> , pages 1941–1942.	767
718		768
719		769
720		770
721		771
722		772
723	Pekka Malo, Ankur Sinha, Pekka Korhonen, Jyrki Wallenius, and Pyy Takala. 2014. Good debt or bad debt: Detecting semantic orientations in economic texts. <i>Journal of the Association for Information Science and Technology</i> , 65(4):782–796.	773
724		774
725		775
726		776
727		777
728	Xiangdi Meng, Damai Dai, Weiyao Luo, Zhe Yang, Shaoxiang Wu, Xiaochen Wang, Peiyi Wang, Qingxiu Dong, Liang Chen, and Zhifang Sui. 2024. Periodiclora: Breaking the low-rank bottleneck in lora optimization. <i>arXiv preprint arXiv:2402.16141</i> .	778
729		779
730		780
731		781
732		782
733	Colin Raffel, Noam Shazeer, Adam Roberts, Katherine Lee, Sharan Narang, Michael Matena, Yanqi Zhou, Wei Li, and Peter J Liu. 2020. Exploring the limits of transfer learning with a unified text-to-text transformer. <i>Journal of machine learning research</i> , 21(140):1–67.	783
734		784
735		785
736		786
737		787
738		788
739	Adithya Renduchintala, Tugrul Konuk, and Oleksii Kuchaiev. 2023. Tied-lora: Enhancing parameter efficiency of lora with weight tying. <i>arXiv preprint arXiv:2311.09578</i> .	789
740		790
741		791
742		792
	Julio Cesar Salinas Alvarado, Karin Verspoor, and Timothy Baldwin. 2015. Domain adaption of named entity recognition to support credit risk assessment. In <i>Proceedings of the Australasian Language Technology Association Workshop 2015</i> , pages 84–90, Parramatta, Australia.	793
		794
		795
		796
	Noam Shazeer. 2020. Glu variants improve transformer. <i>arXiv preprint arXiv:2002.05202</i> .	
	Shuhua Shi, Shaohan Huang, Minghui Song, Zhoujun Li, Zihan Zhang, Haizhen Huang, Furu Wei, Weiwei Deng, Feng Sun, and Qi Zhang. 2024. Reslora: Identity residual mapping in low-rank adaption. <i>arXiv preprint arXiv:2402.18039</i> .	
	Ankur Sinha and Tanmay Khandait. 2021. Impact of news on the commodity market: Dataset and results. In <i>Advances in Information and Communication: Proceedings of the 2021 Future of Information and Communication Conference (FICC), Volume 2</i> , pages 589–601. Springer.	
	Jianlin Su, Murtadha Ahmed, Yu Lu, Shengfeng Pan, Wen Bo, and Yunfeng Liu. 2024. Roformer: Enhanced transformer with rotary position embedding. <i>Neurocomputing</i> , 568:127063.	
	Alex Wang, Amanpreet Singh, Julian Michael, Felix Hill, Omer Levy, and Samuel R Bowman. 2018. Glue: A multi-task benchmark and analysis platform for natural language understanding. <i>arXiv preprint arXiv:1804.07461</i> .	
	Yizhong Wang, Hamish Ivison, Pradeep Dasigi, Jack Hessel, Tushar Khot, Khyathi Chandu, David Wadden, Kelsey MacMillan, Noah A Smith, Iz Beltagy, et al. 2024. How far can camels go? exploring the state of instruction tuning on open resources. <i>Advances in Neural Information Processing Systems</i> , 36.	
	Shijie Wu, Ozan Irsoy, Steven Lu, Vadim Dabravolski, Mark Dredze, Sebastian Gehrmann, Prabhanjan Kambar, David Rosenberg, and Gideon Mann. 2023. Bloomberggpt: A large language model for finance. <i>arXiv preprint arXiv:2303.17564</i> .	
	Longhui Yu, Weisen Jiang, Han Shi, Jincheng Yu, Zhengying Liu, Yu Zhang, James T Kwok, Zhenguang Li, Adrian Weller, and Weiyang Liu. 2023. Metamath: Bootstrap your own mathematical questions for large language models. <i>arXiv preprint arXiv:2309.12284</i> .	
	Biao Zhang and Rico Sennrich. 2019. Root mean square layer normalization. <i>Advances in Neural Information Processing Systems</i> , 32.	
	Chunting Zhou, Pengfei Liu, Puxin Xu, Srinivasan Iyer, Jiao Sun, Yuning Mao, Xuezhe Ma, Avia Efrat, Ping Yu, Lili Yu, et al. 2024. Lima: Less is more for alignment. <i>Advances in Neural Information Processing Systems</i> , 36.	

797 Jiacheng Zhu, Kristjan Greenewald, Kimia Nadjahi,
798 Haitz Sáez de Ocáriz Borde, Rickard Brüel Gabriels-
799 son, Leshem Choshen, Marzyeh Ghassemi, Mikhail
800 Yurochkin, and Justin Solomon. 2024. Asymmetry
801 in low-rank adapters of foundation models. *arXiv*
802 *preprint arXiv:2402.16842*.

A Hyperparameters

We propose hyperparameters in Table 5.

Dataset	Method	r	α	LR	LR Scheduler	Warmup	Epochs	Batch size	$f_{\text{comp}}, f_{\text{decomp}}$
Tülu v2	FFT	-	-	2e-5	cosine	500	2	128	-
	LoRA-like	8	16	{1e-4,2e-4}	cosine	500	2	128	-
	MoRA	8	-	{2e-4,3e-4}	cosine	500	2	128	Eq. 9
	LoRA-like	256	128	{1e-4,2e-4}	cosine	500	2	128	-
	MoRA	256	-	{3e-5,5e-5}	cosine	500	2	128	Eq. 6
MetaMath	FFT	-	-	2e-5	cosine	300	3	128	-
	LoRA-like	8	16	{1e-4,2e-4}	cosine	300	3	128	-
	MoRA	8	-	{2e-4,3e-4}	cosine	300	3	128	Eq. 9
	LoRA-like	256	128	{1e-4,2e-4}	cosine	300	3	128	-
	MoRA	256	-	{3e-5,5e-5}	cosine	300	3	128	Eq. 6
BioMed./Fiance	FFT	-	-	3e-5	linear	150	1	128	-
	LoRA-like	8	16	{3e-4,4e-4}	linear	150	1	128	-
	MoRA	8	-	{4e-4,5e-4}	linear	150	1	128	Eq. 9
	LoRA-like	256	128	{3e-4,4e-4}	linear	150	1	128	-
	MoRA	256	-	{5e-5,7e-5}	linear	150	1	128	Eq. 6

Table 5: Hyperparameters for fine-tuning on three datasets.

B Implementation of ReMoRA

We introduce detail implementation of ReMoRA in pretraining. In this case, we simply define two kinds of g . The first kind is grouping every adjacent \hat{r} rows or columns together following the defined in fine-tuning, the first groups can be represented as $\{1, 2, \dots, \hat{r}\}$. The second kind is grouping every neighboring k of the rows or columns together, the first groups can be represented as $\{1, 1+k, \dots, 1+\hat{r}k\}$. We propose a example code about compression and decompression functions in Algorithm 1 and 2. After merging, we can change the group type from 0 to 1 or 1 to 0.

Algorithm 1 Compression

```

1: function COMPRESS( $x, \hat{r}, type$ )
2:   #  $x \in \mathbb{R}^{bsz \times l \times k}$ : Input tensor
3:   #  $y \in \mathbb{R}^{bsz \times l \times \hat{r}}$ : Output tensor
4:   #  $type \in \{0, 1\}$ : Group type 0 or 1
5:   padding  $x$  to make  $k$  divisible by  $\hat{r}$ 
6:   if  $type = 0$  then
7:      $y = x.view(bsz, l, k/\hat{r}, \hat{r}).sum(dim=2)$  # first type of group
8:   else
9:      $y = x.view(bsz, l, \hat{r}, k/\hat{r}).sum(dim=3)$  # second type of group
10:  end if
11:  return  $y$ 
12: end function

```

Algorithm 2 Decompression

```

1: function DECOMPRESS( $x, \hat{r}, type$ )
2:   #  $x \in \mathbb{R}^{bsz \times l \times \hat{r}}$ : Input tensor
3:   #  $y \in \mathbb{R}^{bsz \times l \times d}$ : Output tensor
4:   #  $type \in \{0, 1\}$ : Group type 0 or 1
5:   if  $type = 0$  then
6:      $y = repeat(x, d/\hat{r}, dim=2)$  # first type of group
7:   else
8:      $y = repeat-interleave(x, d/\hat{r}, dim=2)$  # second type of group
9:   end if
10:  truncate  $y$  to  $\mathbb{R}^{bsz \times l \times d}$ 
11:  return  $y$ 
12: end function

```

C Downstream Tasks of Continual Pretraining

For biomedicine, we use PubMedQA (Jin et al., 2019), RCT (Dernoncourt and Lee, 2017), USMLE (Jin et al., 2021), and selecting biomedicine subjects from MMLU to evaluate the performance. For finance, following BloombergGPT (Wu et al., 2023), we use ConvFinQA (Chen et al., 2022), NER (Salinas Alvarado et al., 2015), Headline (Sinha and Khandait, 2021), FiQA SA (Maia et al., 2018) and FPB (Malo et al., 2014). We report the detail performance of these tasks following:

	r	PubMedQA	USMLE	BioMMLU	RCT	Avg.
FFT	-	74.1	41.2	47.5	62.7	56.4
LoRA	8	73.1	34.9	45.3	54.9	51.9
MoRA	8	73.3	34.7	45.3	59.9	53.3
LoRA	256	73.8	39.7	46.0	56.9	54.1
MoRA	256	74.4	40.4	46.1	60.6	55.4

Table 6: Performance on biomedical tasks.

	r	ConvFinQA	FiQA SA	Headline	NER	FPB	Avg.
FFT	-	44.4	78.8	82.3	68.1	74.3	69.6
LoRA	8	44.5	76.2	72.4	61.6	65.1	64.0
MoRA	8	45.8	76.6	76.3	68.9	68.2	67.1
LoRA	256	41.4	78.3	83.0	66.8	66.7	67.3
MoRA	256	47.7	76.3	83.4	68.0	68.1	68.7

Table 7: Performance on financial tasks.